

## Texture evolution and its simulation of cold drawing copper wires produced by continuous casting

CHEN Jian<sup>1,2</sup>, YAN Wen<sup>1,2</sup>, LI Wei<sup>3</sup>, MIAO Jian<sup>4</sup>, FAN Xin-hui<sup>2</sup>

1. Department of Applied Physics, Northwestern Polytechnical University, Xi'an 710072, China;

2. School of Materials Science and Chemical Engineering, Xi'an Technological University, Xi'an 710032, China;

3. Baoji Titanium Industry Co., Ltd., Baoji 721014, China;

4. School of Materials Science and Engineering, Xi'an Jiaotong University, Xi'an 710049, China

Received 1 January 2010; accepted 14 April 2010

**Abstract:** The texture evolution of cold drawing copper wires produced by continuous casting was measured by X-ray diffractometry and electron back-scatter diffractometry, and was simulated using Taylor model. The results show that in the drawn poly-crystal copper wires produced by traditional continuous casting,  $\langle 111 \rangle$  and  $\langle 100 \rangle$  duplex fiber texture forms, and with increasing strain, the intensities of  $\langle 111 \rangle$  and  $\langle 100 \rangle$  increase. In the drawn single-crystal copper wires produced by Ohno continuous casting,  $\langle 100 \rangle$  rotates to  $\langle 111 \rangle$ , and there is inhomogeneous distribution of fiber texture along radial direction of the wires, which is caused by the distribution of shear deformation. Compared with  $\langle 100 \rangle$ ,  $\langle 111 \rangle$  fiber texture is more stable in the drawn copper wires. Comparison of the experimental results with the simulated results shows that the simulation by Taylor model can analyze the texture evolution of drawn copper wires.

**Key words:** cold drawing; copper wires; texture; Taylor model

### 1 Introduction

During plastic deformation process, usually, crystal rotation takes place and crystal defect forms, which makes the change of microstructures and textures of deformation metals. Actually, many researchers have focused on the texture evolution during deformation process, which is due to the following reasons: 1) The deformation texture significantly affects the properties of deformation metals; 2) The behavior of recovery and recrystallization is closely connected with the deformation texture; 3) Deformation mechanism can be analyzed by the study of deformation texture.

With the development of information technology, the demand of finer copper wires has kept rising. Metallic wire drawing technology has advanced possibility of manufacturing the fine wires with a diameter less than 20  $\mu\text{m}$ [1]. Therefore, texture evolution of drawn copper wires has been widely investigated using X-ray diffractometry (XRD), neutron

diffractometry or electron back-scatter diffractometry (EBSD)[2–4]. It has been reported that the cold drawing copper wires have typical textures consisting of a majority  $\langle 111 \rangle$  and a minority  $\langle 100 \rangle$ [2, 4]. ENGLISH and CHIN[5] found that the relative intensity ratio of  $\langle 111 \rangle$  and  $\langle 100 \rangle$  fiber texture is different from one material to others and depends on their stacking fault energy. The texture evolution in drawn copper wires is affected by the deformation temperature, and the intensity ratio of  $\langle 100 \rangle$  to  $\langle 111 \rangle$  is larger at  $-196$ ,  $-77$  or  $100$  °C than that at  $0$  °C[6], which is due to the depletion of  $\langle 111 \rangle$  by twinning at low temperature and by recrystallization at high temperature. Although much work has been done on fiber texture evolution of cold drawn copper wires, the study object is the annealing copper wires and very little work has been paid attention to the texture evolution of the copper wires produced by continuous casting, especially, the single crystal copper wires produced by Ohno continuous casting (OCC)[7–10]. In the present work, therefore, the texture evolution of cold drawn copper wires produced by continuous casting was

analyzed by XRD and EBSD, and simulated by Taylor model.

## 2 Experimental

Polycrystal and single crystal copper wires with a diameter of 8 mm were produced by use of traditional continuous casting technique and OCC method, respectively. During the cold drawn processing, the deformed copper wires were not annealed, and to eliminate the effect of drawn direction on the texture evolution, the drawn directions were kept same in every time of drawing. The true strain of drawn copper wires can be calculated by following equation:

$$\varepsilon = \ln \frac{A_0}{A} = 2 \ln \frac{d_0}{d} \quad (1)$$

where  $\varepsilon$  indicates true strain of the drawn wires;  $A_0$  and  $d_0$  denote initial cross-section and diameter, respectively; and  $A$  and  $d$  are those of the drawn wires. Texture measurement of cold drawn polycrystal copper was carried out on D/max-III XRD and the samples for XRD were cut according to Fig. 1. The texture of single crystal copper was analyzed on a FEI Quanta-400F thermal FEG scanning electron microscope with HKL Channel 5 system at 20 kV. Samples for EBSD were polished mechanically, and then electropolished in a solution of 500 mL distilled water, 250 mL  $\text{HPO}_3$ , 250 mL ethanol, 50 mL propanal and 5 g carbamide at 4 V and  $-15^\circ\text{C}$  for 4 min.

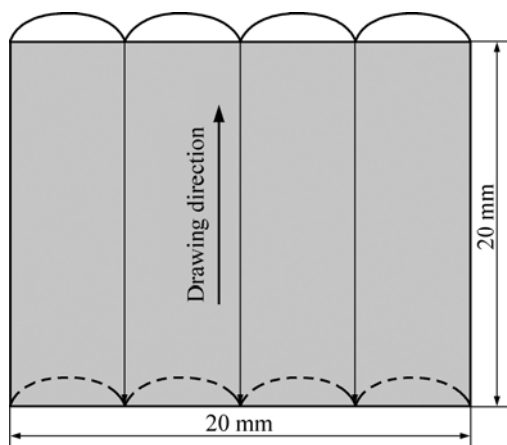


Fig.1 Sample for XRD analysis

## 3 Results and discussion

### 3.1 Copper wires without deformation

In traditional continuous casting technique, because the heat flows from the center to the surface of the copper wires, crystal nuclei, which form on the surface of the wires due to cold mould, grow from the surface to the center of the wires. Therefore, columnar crystal

perpendicular to axis direction of wires can be observed, as shown in Fig.2(a). However, the temperature gradient can be ignored in the center of wires, and then the grains in the center are equiaxed, as shown in Fig.2(b). Fig.2(c) shows  $\{100\}$  pole figure of polycrystalline copper wires produced by traditional continuous casting technique, indicating that the wires can be considered grains with weak initial texture.

In OCC method[7], to prevent the nucleation of crystals on the mould wall, a heated mould instead of the conventional cold mould is used to maintain a certain temperature. There is competitive growth of grains at the initial solidification stage of OCC method, due to convex solid/liquid interfaces. Competitive growth of grains

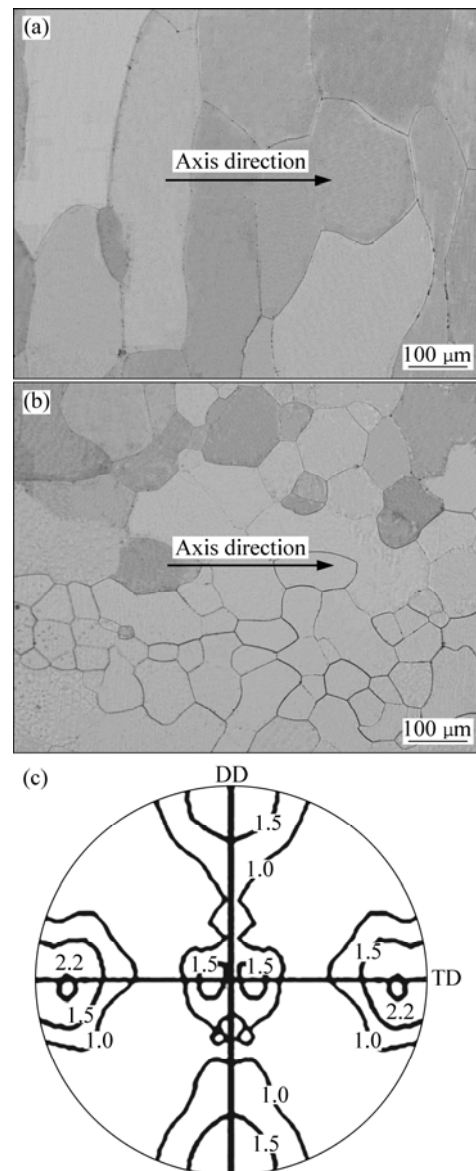


Fig.2 Microstructure and texture of copper wires produced by traditional continuous casting technique: (a) Near surface; (b) At center; (c)  $\{100\}$  pole figure (DD indicates drawing direction and TD represents transverse direction)

means those grains with a high angle between  $\langle 100 \rangle$  and the direction of heat flow, the axial direction of the wires will be swallowed by those with a low angle. Thus, the axial direction of the single crystal copper wires produced by OCC is always close to  $\langle 100 \rangle$ .

**3.2 Texture evolution of drawn copper wires**

Fig.3 shows the orientation map of single crystal copper with different strains. In Fig.3, the crystal directions indicated by color are parallel to the drawing direction of the samples. From Fig.3, it can be found that at a strain of 0.28, the orientation of drawn single crystal copper referred to drawn direction does not change and is still close to  $\langle 100 \rangle$ . At strains between 0.58 and 1.96, although the axis direction of some regions in drawn single crystal copper deviates from  $\langle 100 \rangle$ ,  $\langle 111 \rangle$  fiber texture component cannot be observed. When the strain is more than 1.96,  $\langle 111 \rangle$  and  $\langle 100 \rangle$  duplex fiber texture forms, and with increasing strains, the intensity of  $\langle 111 \rangle$  fiber texture increases. According to Figs.3(a)–(c), it can be found that at low strains, besides of  $\langle 100 \rangle$  fiber texture  $\langle 112 \rangle$  can be observed, indicating that  $\langle 100 \rangle$  rotates to  $\langle 111 \rangle$  through  $\langle 112 \rangle$ . When strain is more than 2.77, inhomogeneous distribution of fiber texture in the wires appears. At a strain of 2.77, a large number of regions with  $\langle 111 \rangle$  fiber texture component are in the centre of the wires. Increasing the strain to 4.12,  $\langle 111 \rangle$  fiber texture component spreads from the center to the surface and the middle regions of deformed samples compared with the specimens with a strain of 2.77.

Fig.4 shows the  $\{100\}$  pole figure of drawn

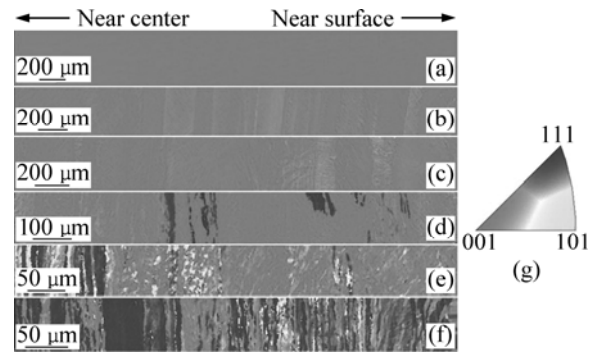


**Fig.3** Orientation map for longitudinal section samples of drawn  $\langle 100 \rangle$  single crystal copper wires with strains of 0.28 (a), 0.58 (b), 0.94 (c), 1.96 (d), 2.77 (e) and 4.12 (f) referred to drawing direction, and key (g)

polycrystalline copper wires with different strains. From Fig.4, it can be found that the deformation textures of drawn polycrystalline copper wires produced by traditional continuous casting can be characterized as the major  $\langle 111 \rangle$  and minor  $\langle 100 \rangle$  duplex fiber texture parallel to drawn direction. When the true strain is low,  $\langle 001 \rangle$  and  $\langle 111 \rangle$  fiber texture components are diffused. With the increase of true strain, the diffuse degree of  $\langle 001 \rangle$  and  $\langle 111 \rangle$  fiber texture components decreases.

In FCC metals with medium or high stacking fault energy, many studies[11–14] have proved that the deformation textures consisting of  $\langle 111 \rangle$  and  $\langle 100 \rangle$  duplex fiber texture parallel to drawing direction forms during cold drawing process. Therefore,  $\langle 111 \rangle$  and  $\langle 100 \rangle$

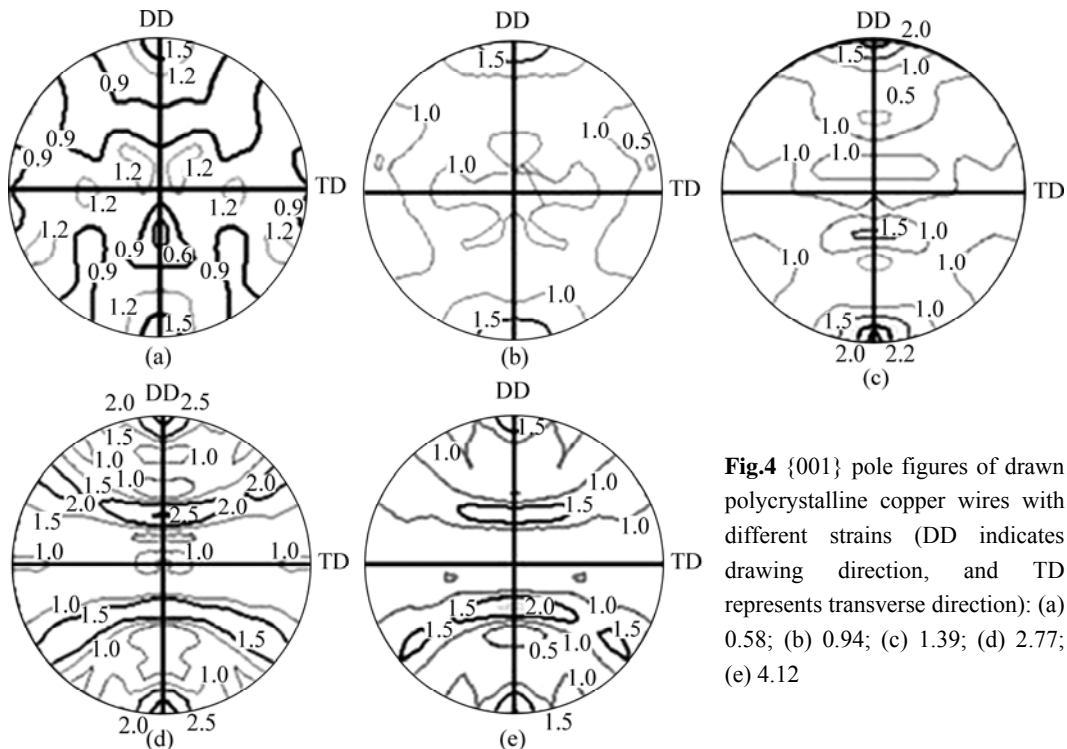


**Fig.4**  $\{001\}$  pole figures of drawn polycrystalline copper wires with different strains (DD indicates drawing direction, and TD represents transverse direction): (a) 0.58; (b) 0.94; (c) 1.39; (d) 2.77; (e) 4.12

can be considered final stable fiber textures in drawn FCC metals with medium or high stacking fault energy. In the present work, for drawn polycrystalline copper wires produced by traditional continuous casting,  $\langle 111 \rangle$  and  $\langle 100 \rangle$  duplex fiber textures can be observed at high strains, which are consistent with the results of previous studies[11–14]. When the initial orientation is one of final stable fiber textures, for example, the initial orientation of single crystal copper wires produced by OCC is  $\langle 100 \rangle$  parallel to drawing direction, the crystal still is not stable, and  $\langle 100 \rangle$  rotates to  $\langle 111 \rangle$  through  $\langle 112 \rangle$ . At high strains,  $\langle 111 \rangle$  and  $\langle 100 \rangle$  duplex fiber textures form. In addition, at high strains,  $\langle 111 \rangle$  fiber texture spreads from the center to the surface of the wires with increasing strain in drawn single crystal copper with initial orientation  $\langle 100 \rangle$  parallel to drawing direction, indicating that there is inhomogeneous distribution of fiber texture, which should be resulted from inhomogeneous distribution of shear strain. CHO et al[15] proposed by finite element analysis that there is a variation of shear strain with radial position, which comes from geometry deformation and friction effect, and the shear strain increases with the increase distance from the center of the wires. The spread of  $\langle 111 \rangle$  fiber texture from the center to the surface with increasing strain in drawn  $\langle 100 \rangle$  single crystal copper indicates that shear deformation is not beneficial to the formation of  $\langle 111 \rangle$  fiber texture parallel to drawn direction.

#### 4 Simulation of cold drawn texture

In the present work, Taylor model[16] is used to simulate the texture evolution during cold drawing process. In Taylor model, it is considered that each grain is with same strain. During cold drawing process, the strain tensor  $\mathbf{L}'_{ij}$  in sample reference frame can be expressed as[17]

$$\mathbf{L}'_{ij} = \begin{Bmatrix} \varepsilon & 0 & 0 \\ 0 & -\varepsilon/2 & 0 \\ 0 & 0 & -\varepsilon/2 \end{Bmatrix} \quad (2)$$

where  $\varepsilon=2\ln R/R'$ .  $R$  and  $R'$  indicate the diameters of before and after deformation wires.

The strain tensor  $\mathbf{L}_{ij}$  in crystal reference frame can be expressed as

$$\mathbf{L}_{ij} = \sum_k m_{ij}^k \gamma_k + \boldsymbol{\Omega}_{ij} \quad (3)$$

where  $\gamma_k$  is the shear rate for  $k$  slipping system;  $\boldsymbol{\Omega}_{ij}$  is the rotation tensor of the deformation crystal;  $m_{ij}^k = \mathbf{b}^k \times \mathbf{n}^k$ , and  $\mathbf{b}^k$  and  $\mathbf{n}^k$  are the normalization vectors of the slipping direction and the normal direction of slipping plane for  $k$

slipping system, respectively.

During deformation process, the strain tensor  $\mathbf{L}_{ij}$  can also be expressed as[18]

$$\mathbf{L}_{ij} = \mathbf{D}_{ij}^s + \mathbf{D}_{ij}^a \quad (4)$$

$$\mathbf{D}_{ij}^s = \frac{1}{2}(\mathbf{L}_{ij} + \mathbf{L}_{ij}^T) = \sum_{k=1}^m \frac{1}{2} \gamma_k (\mathbf{b}^k \mathbf{n}^k + \mathbf{n}^k \mathbf{b}^k) \quad (5)$$

$$\mathbf{D}_{ij}^a = \frac{1}{2}(\mathbf{L}_{ij} - \mathbf{L}_{ij}^T) = \sum_{k=1}^m \frac{1}{2} \gamma_k (\mathbf{b}^k \mathbf{n}^k - \mathbf{n}^k \mathbf{b}^k) + \boldsymbol{\Omega}_{ij} \quad (6)$$

In Eqs.(4)–(6),  $\mathbf{D}_{ij}^s$  and  $\mathbf{D}_{ij}^a$  are symmetrical strain tensor and asymmetry strain tensor, respectively.

In order to simulate the texture evolution, the rotation tensor  $\boldsymbol{\Omega}_{ij}$  must be obtained from Eq.(6). The relationship between the strain tensor  $\mathbf{L}_{ij}$  in crystal reference frame and the strain tensor  $\mathbf{L}'_{ij}$  in sample reference frame is

$$\mathbf{L}_{ij} = \mathbf{T}' \mathbf{L}'_{ij} \mathbf{T} \quad (7)$$

$\mathbf{L}'_{ij}$  can be obtained from Eq.(7);  $\mathbf{T}$  is orientation matrix of crystals before deformation.

$$\mathbf{T} = \begin{Bmatrix} u & r & h \\ v & s & k \\ w & t & l \end{Bmatrix} \quad (8)$$

where  $\{hkl\}$  is perpendicular to the normal direction of analyzed planes;  $\langle uvw \rangle$  is parallel to drawing direction and  $[rst] = [hkl] \times [uvw]$ . Therefore, the strain tensor  $\mathbf{L}_{ij}$  in crystal reference frame and the shear rate  $\gamma_k$  can be obtained from Eqs.(7) and (5), respectively. If  $\mathbf{L}_{ij}$ ,  $\gamma_k$ ,  $\mathbf{b}^k \mathbf{n}^k$  and  $\mathbf{n}^k \mathbf{b}^k$  are substituted into Eq.(6), the value of  $\boldsymbol{\Omega}_{ij}$  will be known. Then, the orientation matrix of crystals after deformation can be calculated from the following equation[19]:

$$\mathbf{F} = (\mathbf{I} - \boldsymbol{\Omega}_{ij}) \mathbf{T} \quad (9)$$

where  $\mathbf{I}$  is the unit matrix.

According to above method, the texture evolution of copper wires produced by OCC method and traditional continuous casting can be simulated. During simulating process, the wires produced by traditional continuous casting and OCC method are considered grains without any initial texture and with  $\langle 100 \rangle$  parallel to drawing direction, respectively. Fig.5 shows  $\{100\}$  pole figures of drawn polycrystalline copper wires with different strains. From Fig.5, it can be found that after cold drawing deformation,  $\langle 111 \rangle$  and  $\langle 100 \rangle$  duplex fiber texture forms in polycrystalline copper wires without any initial texture. With increasing strain the intensities of  $\langle 111 \rangle$  and  $\langle 100 \rangle$

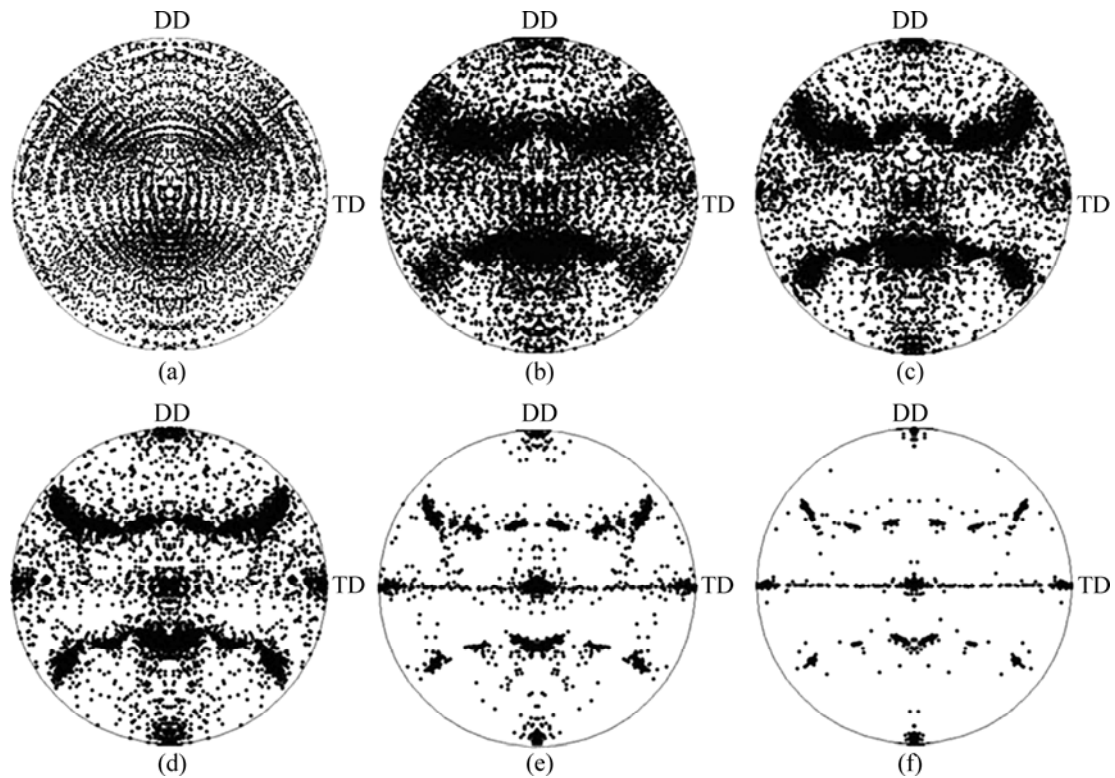


**Fig.5** {001} pole figures of cold drawn polycrystalline copper wires simulated by Taylor model: (a) 0.28; (b) 0.58; (c) 0.94; (d) 1.39; (e) 2.77; (f) 4.12

increase. Comparison of the results in Fig.2 and Fig.4 with the results in Fig.5 shows that although there is little difference between initial orientation of measured copper wires and that of simulation metals, i.e. the measured copper wires have a weak preferred orientation and simulation metals are without any initial texture. The simulation results of drawn copper wires are very similar to the measured those of drawn polycrystalline copper wires, especially at high true strains, indicating that the effect of initial crystal orientation of drawn polycrystalline copper wires on final drawn texture can be ignored.

Fig.6 shows {100} pole figures of cold drawn copper wires with initial orientation  $\langle 100 \rangle$  parallel to drawing direction. From Fig.6, it can be seen that  $\langle 111 \rangle$  and  $\langle 100 \rangle$  duplex fiber texture forms in the drawn copper wires with initial orientation  $\langle 100 \rangle$  parallel to drawn direction and  $\langle 100 \rangle$  rotates to  $\langle 111 \rangle$ , which is agreement with the experimental results of drawn copper wires produced by OCC method (see Fig.3). However, comparison of the results in Fig.6 with those in Fig.3 shows that there is a difference between the texture evolution simulated by Taylor model and that measured by EBSD. For example, in the results simulated by Taylor model (see Fig.6), at a strain of 0.28, the rotation

degree of crystal is great. In contrast, for single crystal copper wires produced by OCC method, at a strain of 0.28, the orientation of drawn single crystal copper referred to drawn direction does not change and is still close to  $\langle 100 \rangle$  (see Fig.3). Actually, the simulated wires without deformation are considered  $\langle 100 \rangle$  parallel to drawing direction, but other crystal directions are not determined. Then, they still are poly-crystal, as shown in Fig.6(a). The wires produced by OCC method are single crystal and  $\langle 100 \rangle$  is parallel to drawing direction, as shown in Fig.3(a). Thus, there is a difference of grain size between the wires simulated by Taylor model and measured by EBSD, indicating that the grain size affects texture evolution of cold drawn copper wires. In addition, previous studies[2–4] have proved that  $\langle 111 \rangle$  and  $\langle 100 \rangle$  are final stable fiber texture in FCC metals with medium or high stacking fault energy. In the present work, the results measured by EBSD and simulated by Taylor model show that  $\langle 100 \rangle$  rotates to  $\langle 111 \rangle$  in copper wires with initial orientation  $\langle 100 \rangle$  parallel to drawing direction, and the intensity of  $\langle 111 \rangle$  is more than that of  $\langle 100 \rangle$  in drawn polycrystalline copper wires with high strains, indicating that compared with  $\langle 100 \rangle$ ,  $\langle 111 \rangle$  fiber texture parallel to drawn direction is more stable in drawn copper wires.

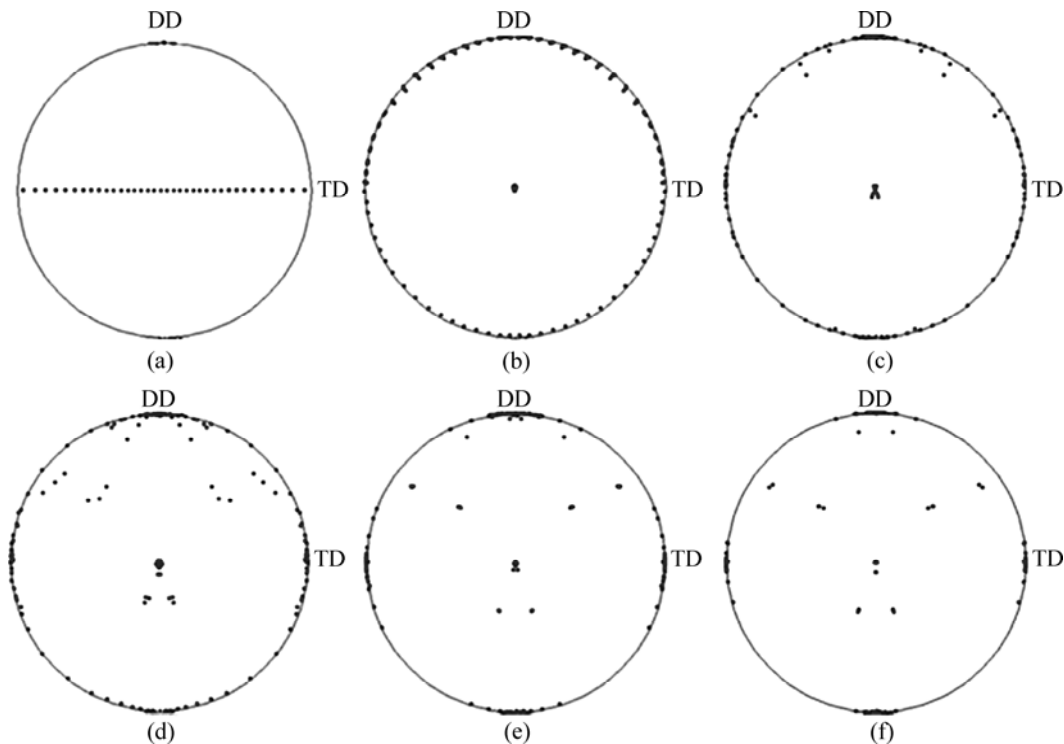


**Fig.6**  $\{100\}$  pole figures of cold drawn copper wires with  $\langle 001 \rangle$  initial orientation simulated by Taylor model: (a) Without deformation; (b) 0.28; (c) 0.58; (d) 1.96; (e) 2.77; (f) 4.12

## 5 Conclusions

1) In drawn polycrystal copper wires produced by traditional continuous casting,  $\langle 111 \rangle$  and  $\langle 100 \rangle$  duplex fiber texture forms, and with increasing strains, the intensities of  $\langle 111 \rangle$  and  $\langle 100 \rangle$  increase.

2) In drawn single-crystal copper wires with initial orientation  $\langle 100 \rangle$  parallel to drawing direction,  $\langle 100 \rangle$  rotates to  $\langle 111 \rangle$ , and  $\langle 111 \rangle$  and  $\langle 100 \rangle$  duplex fiber texture forms at high strains. Compared with  $\langle 100 \rangle$ ,  $\langle 111 \rangle$  fiber texture is more stable in drawn copper wires.

3) Inhomogeneous distribution of fiber texture in drawn single-crystal copper wires along radial direction is caused by the distribution of shear deformation.

## References

- [1] INAKAZU N, KANENO Y, INOUE H. Fiber texture formation and mechanical properties in drawn fine copper wires [J]. *Materials Science Forum*, 1994, 157–162: 715–720.
- [2] GERBER P H, JAKANI S, MATHON M H, BAUDIN T. Neutron diffraction measurements of deformation and recrystallization in cold wire-drawn copper [J]. *Materials Science Forum*, 2005, 495–497: 919–926.
- [3] WULFF F, BREACH C D, DITTMER K. Crystallographic texture of drawn gold bonding wires using electron backscattered diffraction (EBSD) [J]. *J Materials Science Letter*, 2003, 22: 1373–1376.
- [4] RAJIAN K, PETKIE R. Microtexture and anisotropy in wire drawn copper [J]. *Materials Science and Engineering A*, 1998, 257: 185–197.
- [5] ENGLISH A T, CHIN G Y. On the variation of wire texture with stacking fault energy in fcc metals and alloys [J]. *Acta Metall*, 1965, 13: 1013–1016.
- [6] WARYOBAR D R. Deformation and annealing behavior of heavily drawn oxygen free high conductivity copper [D]. Florida: The Florida State University, 2003.
- [7] OHNO A. Continuous casting of single crystal ingots by the O.C.C. process [J]. *Journals of Metals*, 1986, 38: 14–16.
- [8] YAN Wen, CHEN Jian, FAN Xin-hui. Effects of grain boundaries on electrical property of copper wires [J]. *Transactions of Nonferrous Metals Society of China*, 2003, 13(5): 1075–1079.
- [9] CHEN Jian, YAN Wen, WANG Xue-yan, FAN Xin-hui. Microstructure evolution of single crystal copper wires in cold drawing [J]. *Science in China Series E: Technological Sciences*, 2007, 50(6): 736–748.
- [10] SODA H, MCLEAN A, WANG Z, MOTOYASU G. Pilot-scale casting of single-crystal wires by Ohno continuous casting process [J]. *Journal of Materials Science*, 1995, 30: 5438–5448.
- [11] CHO J H, CHO J S, MOON J T, LEE J, CHO Y H, KIM Y W, ROLLETT A D, OH K H. Recrystallization and grain growth of cold-drawn gold bonding wire [J]. *Metallurgical and Materials Transactions A*, 2003, 34: 1113–1125.
- [12] SHIN H J, JEONG H T, LEE D N. Deformation and annealing textures of silver wire [J]. *Materials Science and Engineering A*, 2000, 279: 244–253.
- [13] CHO J H, ROLLETT A D, OH K H. Determination of volume fractions of texture components with standard distributions in Euler

- space [J]. Metallurgical and Materials Transactions A, 2004, 35: 1075–1086.
- [14] CHO J H, ROLLETT A D, CHO J S, PARK Y J, MOON J T, OH K H. Investigation of recrystallization and grain growth of copper and gold bonding wires [J]. Metallurgical and Materials Transactions A, 2006, 37: 3085–3097.
- [15] CHO J H, ROLLETT A D, CHO J S, PARK Y J, OH K H. Investigation on cold-drawn gold bonding wires with serial and reverse-direction drawing [J]. Materials Science and Engineering A, 2006, 432: 202–215.
- [16] TAYLOR G I. Plastic strain in metals [J]. J Inst Met, 1938, 62: 307–324.
- [17] LIU Yan-dong, JIANG Qi-wu, ZHAO Xiang, ZUO Liang, LIANG Zhi-de. Texture analysis and simulation of pearlitic wires during drawing [J]. Acta Metall Sinica, 2002, 38(11): 1215–1218. (in Chinese)
- [18] ZHANG Yao-liang, ZHU Wei-bing. Tensor analysis and its application in continuum mechanics [M]. Harbin: Harbin Engineering University Press, 2004: 72–73. (in Chinese)
- [19] LIU Yan-sheng, XU Jia-zhen, LIANG Zhi-de. Simulation of cold rolling textures of bcc metals [J]. Chinese Journal of Materials Research, 1990, 5(4): 377–380. (in Chinese)

## 连续铸造铜线材冷拔形变织构的演化及计算机模拟

陈建<sup>1,2</sup>, 严文<sup>1,2</sup>, 李巍<sup>3</sup>, 苗健<sup>4</sup>, 范新会<sup>2</sup>

1. 西北工业大学 应用物理系, 西安 710072; 2. 西安工业大学 材料与化工学院, 西安 710032;  
3. 宝鸡钛业有限公司, 宝鸡 721014; 4. 上海交通大学 材料科学与工程学院, 西安 710049

**摘要:** 采用 X 射线衍射以及电子背散射衍射技术分析连续铸造技术制备的铜线材冷拔形变织构的演化, 并采用 Taylor 模型对其进行计算机模拟。结果表明, 采用传统连续铸造技术制备的多晶铜线材经过冷拔变形后形成  $\langle 001 \rangle + \langle 111 \rangle$  丝织构, 随着变形量的增加, 2 种织构组分的强度增加。OCC 技术制备的  $\langle 100 \rangle$  单晶铜线材, 在冷拔变形过程中, 部分区域的  $\langle 100 \rangle$  会向  $\langle 111 \rangle$  转动, 并且剪切应力的不均匀分布将导致形变织构组分沿线材径向不均匀分布。在冷拔织构组分中, 与  $\langle 100 \rangle$  相比,  $\langle 111 \rangle$  织构组分更加稳定。实验结果与模拟结果对比表明, Taylor 模型能够很好地模拟铜线材冷拔形变织构的演化。

**关键词:** 冷拔; 铜线材; 织构; Taylor 模型

(Edited by YANG Hua)